D. ABUBAKAR,[1] N. MAHMOUD,[2] SH. MAHMUD[3]

[1] Physics Department, Bauchi State University Gadau
(65, Itas/Gadau – Bauchi Nigeria; e-mail: dabubakar19@yahoo.com)
[2] Nano-Optoelectronics Research Laboratory (NOR) – School of Physics Universiti Sains Malaysia
(11800 Gelugor Pulau Pinang – Malaysia)
[3] Nano-Optoelectronics Research Laboratory (NOR) – School of Physics, Universiti Sains Malaysia
(11800 Gelugor Pulau Pinang – Malaysia)

INVESTIGATION ON THE STRUCTURAL AND OPTICAL PROPERTIES OF NiO NANOFLAKES. CHEMICAL BATH DEPOSITION OF $Ni(OH)_2$ THIN FILMS

UDC 539

Porous nickel oxide (NiO) nanoflakes are grown by the chemical bath deposition. The thin films are produced on an ITO/glass substrate and annealed at a variable temperature in a furnace. The structural and optical properties and the surface morphology of the thin films are studied and analyzed. FESEM results display the presence of nanoflakes with the structure of $NiO/Ni(OH)_2$ in thin films that appear to increase in size with the annealing temperature. The sample grown at 300 °C is observed to have the highest surface area dimension. The EDX result reveals that the atomic ratio and weight of the treated sample has a non-stoichiometric value, which results in the p-type behavior of the NiO thin film. The result obtained by AFM indicates the highest roughness value (47.9 nm) for a sample grown at 300 °C. The analysis on XRD shows that the NiO nanoflakes possess a cubic structure with the orientation peaks of (111), (200), and (220). This appears with a stronger intensity at 300 °C. Likewise, XRD result approves the absence of the $Ni(OH)_2$ peak at the annealing. For the optical band gap, the UV-Vis measurements give a lower value of 3.80 eV for 300 °C due to the highest crystallinity. The optimum temperature to synthesize high-quality NiO nanoflakes is 300 °C, which can be an important factor for good sensing devices.

Keywords: annealing temperature, nanoflakes, thin film, chemical bath deposition, nickel oxide.

1. Introduction

Nickel oxide (NiO) thin films have attracted much attention by the great chemical stability, high optical density, dynamic range, great electrochemical effect, low-cost material device application, and high chemical durability [1]. Nickel oxide is a semiconductor and, generally, is considered as a model of *p*-type material. Due to the electronic properties of nanostructured NiO such as the wide energy band-gap of 3.6–4.0 eV with high thermal stability, it is qualified to be a favourable material in several applications in nanoelectronic devices such as electrochromic display [2], supercapacitance [3], electrochemical charging/discharging mechanism [4], catalysts [5], and sensor devices [6]. NiO possesses the cubic or rhombohedral structure, but the cubic structure is the most commonly obtained structure [7, 8].

The different applications of NiO thin films are based on their structural and morphological properties. The porous nanostructured thin film offers a wide surface area that can result in a very short pathway for the diffusion of ions. NiO thin films with nanometric pores have been given a much attention because of their novel large surface area and geometry of the interior. The porous nanostructure of NiO thin films has turned out to own a greater performance than their counterparts with compact structure, particularly in applications in electrochemistry [9, 10].

Nowadays, numerous chemical and physical techniques such as the electro-deposition [10], thermal decomposition [11], template synthesis [12], chemical bath deposition (CBD) [13], sol-gel method [14], hydrothermal method [15], spray pyrolysis [16], pulse

laser deposition method (PLD) [17], and anodic electrochemical deposition [18] have been employed to enhance the functionality of nanoporous thin films.

The CBD method is considered as a technique that has an advantage over the other preparation techniques mentioned above because of its convenience in the large surface deposition, low cost, and low-temperature synthesis. The CBD technique involves the substrate insertion into an aqueous solution of a precursor species and the heating to a certain temperature. The required hydroxide is then precipitated and deposited on the surface of the substrate, which results in the production of thin films [19].

2. Experimental

2.1. Sample preparation

The thin layer of nanostructured NiO was deposited,by using the CBD technique. The chemicals used were reagents of analytical grade and were employed with no more purification. Deionized water was utilized in this deposition. The precursor solution for NiO nanoporous thin films was obtained, by using 2.24 g of potassium chloride (KCl) and 2.63 g of nickel sulphate hexahydrate ($NiSO_4 \cdot 6H_2O$) aqueous solutions. Furthermore, 40 ml of a 35% aqueous solution of ammonia was further introduced as a complex agent. The complete solution volume was made to 100 ml by topping with 20 ml of de-ionized water into a beaker 100 ml in volume. The mixture was stirred at 300 rpm for 30 min in order to have solution homogeneity. The layers of the substrates were ultrasonically and chemically cleaned in ethanol, as well as in acetone, each for 15 min, at a 40 °C heating temperature. Then, finally, the substrate was rinsed with deionized water and dried in a nitrogen gas. The substrates were then vertically inserted into the solution and heated inside a laboratory oven at a fixed temperature of 90 °C. Then they were annealed at a variable temperature of 200, 300 and 400 °C inside a furnace to obtain the desired NiO nanoflakes thin film.

2.2. Mechanisms

The chemical reactions of ions involved in the growth of $Ni(OH)_2$ nanoflakes can be seen as follows. In the aqueous solution of hydrated nickel (II) sulphate, the stable solution was obtained with green as a result of the presence of $[Ni(OH_2)_6]^{2+}_{(aq)}$ ions (hexaaqua nickel (II)) in the solution [20]. Ni^{2+} ions present in the solution react with Cl^- ions (ligand) to forms a $[NiCl_4]^{2-}$ ionic complex (tetrachloronickelate (II)) from $KCl_{(aq)}$. The oxy-hydroxide presence was because of the precursor solution of potassium chloride, which is a complex agent resulting into the $Ni(OH)_2$ thin film formation

$$[Ni(OH_2)_6]^{2+}_{(aq)} + 4Cl^-_{(aq)} \rightleftharpoons [NiCl_4]^{2-}_{(aq)} + 6H_2O_{(l)}.$$

With the addition of an ammonia ligand excess aqueous solution, the mixture that contains the $[NiCl_4]^{2-}_{(aq)}$ ions (yellowish-green tetrachloronickelate (II)) and $[Ni(H_2O)_6]^{2+}_{(aq)}$ (ion pale-green stable hexaaqua nickel(II)) reacts to form the $([Ni(NH_3)_6]^{2+}_{(aq)}$ ion complex (hexammine blue-violet solution), which is a substitution reaction of typical ligand [21]

$$[NiCl_4]^{2-}_{(aq)} + 6NH_{3(aq)} \rightleftharpoons [Ni(NH_3)_6]^{2+}_{(aq)} + 4Cl^-_{(aq)},$$

$$[Ni(OH_2)_6]^{2+}_{(aq)} + 6NH_{3(aq)} \rightleftharpoons [Ni(NH_3)_6]^{2+}_{(aq)} + 6H_2O_{(l)}.$$

The precipitation of blue-violet was observed at the interface due to the hydroxide ion and nickel (II) ion reaction from the ammonia hydrolysis with a basic solution

$$Ni^{2+}_{(aq)} + 2OH^-_{(aq)} \rightleftharpoons Ni(OH)_{2(s)},$$

$$NH_{3(aq)} + H_2O_{(l)} \rightleftharpoons NH^+_{4(aq)} + OH^-_{(aq)}.$$

The $[Ni(NH_3)_6]^{2+}$ and $[NiCl_4]^{2-}$ complexes are then hydrolyzed because of the high OH^- concentration, which reduces the $Ni(OH)_{2(s)}$ insoluble pale green solid precipitate formation at the 90 °C heating temperature. This substance is known as an amphoteric substance, since it can be formed by the OH^- ion (hydroxide) addition that results in the formation of a soluble salt of Ni^{2+} ion. Finally, a $Ni(OH)_2$ thin-film layer is deposited on the substrate as shown below:

$$[Ni(NH_3)_6]^{2+} + OH^-_{(aq)} \rightleftharpoons Ni(OH)_{2(s)} + NH_{3(aq)},$$

$$[NiCl_4]^{2-} + OH^-_{(aq)} \rightleftharpoons Ni(OH)_{2(s)} + 4Cl^-.$$

The substrate was then washed with deionized water after the thin film deposition in order to detached $Ni(OH)_2$ particles, which are weakly bonded, and dried with a nitrogen gas flow. The thin films appear pale-green, which indicates a solid thin deposited layer of $Ni(OH)_2$. The thickness of the as-grown $Ni(OH)_2$ deposited thin film was measured to

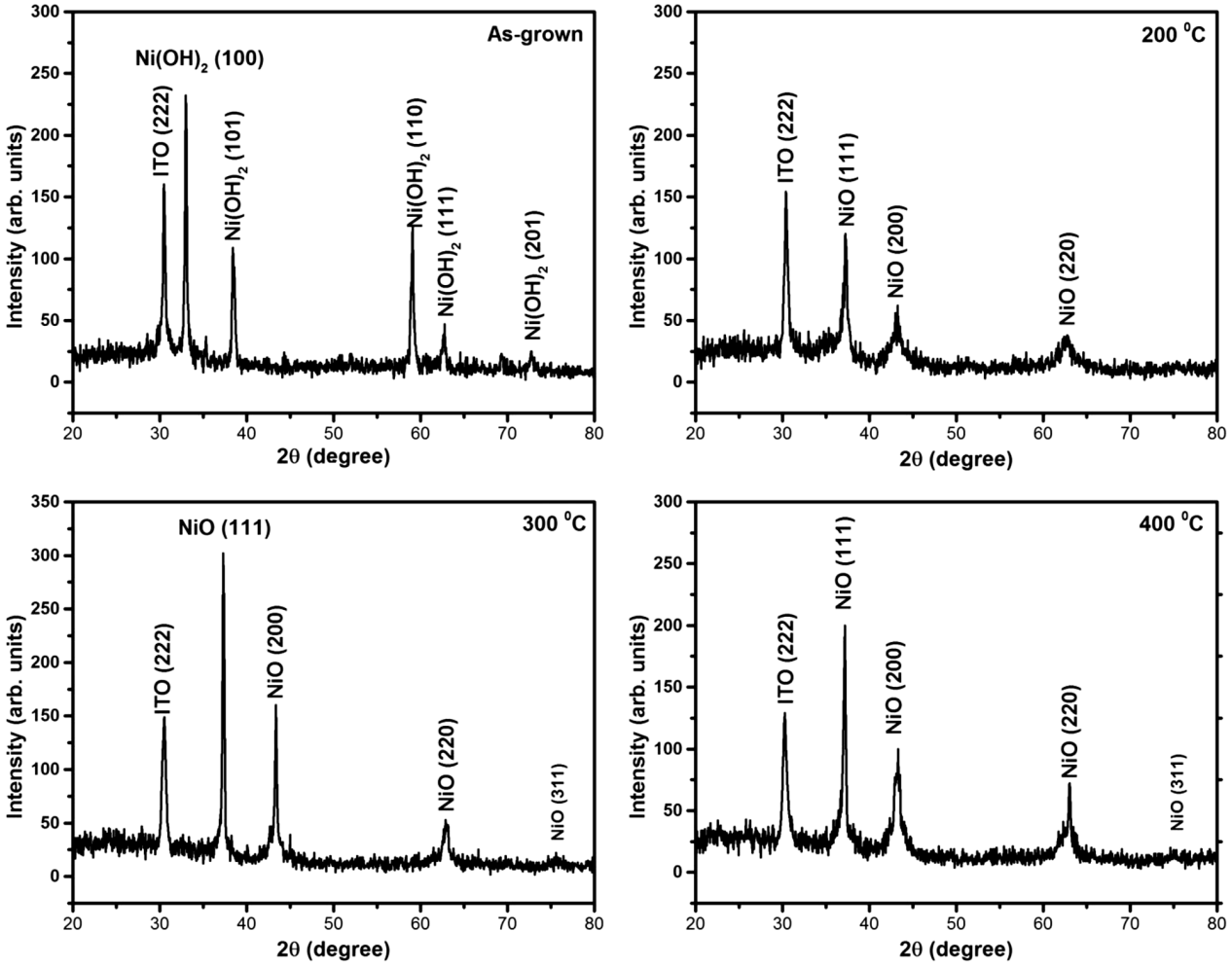

Fig. 1. XRD peaks for the as-grown $Ni(OH)_2$ sample of NiO and samples annealed at different temperatures

be about 1013 nm. The synthesis procedure for NiO was based on the $Ni(OH)_2$ thermal decomposition to produce a nanostructured NiO thin film, as shown in the reaction below:

$$Ni(OH)_2 \rightleftharpoons NiO + H_2O.$$

To find the optimum temperature of the synthesis of NiO thin films from the as-grown $Ni(OH)_2$, three samples were annealed at 200, 300 and 400 °C in a furnace for 90 min for the growth of desired NiO thin films.

2.3. Characterization techniques

The analysis of X-ray diffraction patterns was made, by using a high-resolution X-ray diffraction system (Model: Panalytical X'Pert PRO MRD PW3040) equipped with CuKα (1.5406 Å) radiation. To study the surface physical morphology and roughness, an Atomic Force Microscope (AFM) Veeco NanoScope Analysis version 1.2 (Model: Dimension EDGE, BRUKER) Atomic force microscopy (AFM) was used; a field-emission scanning electron microscope (FESEM Model: FEI Nova NanoSEM 450) was employed to analyze the nanostructure of thin films; and a UV-VIS-NIR spectrometer (Jobin Yvon HR 800 UV) was used to investigate the optical properties of the obtained thin film layer.

3. Results and Discussion

X-ray diffraction patterns and the related peaks of chemically grown nanoporous NiO are shown in Fig. 1

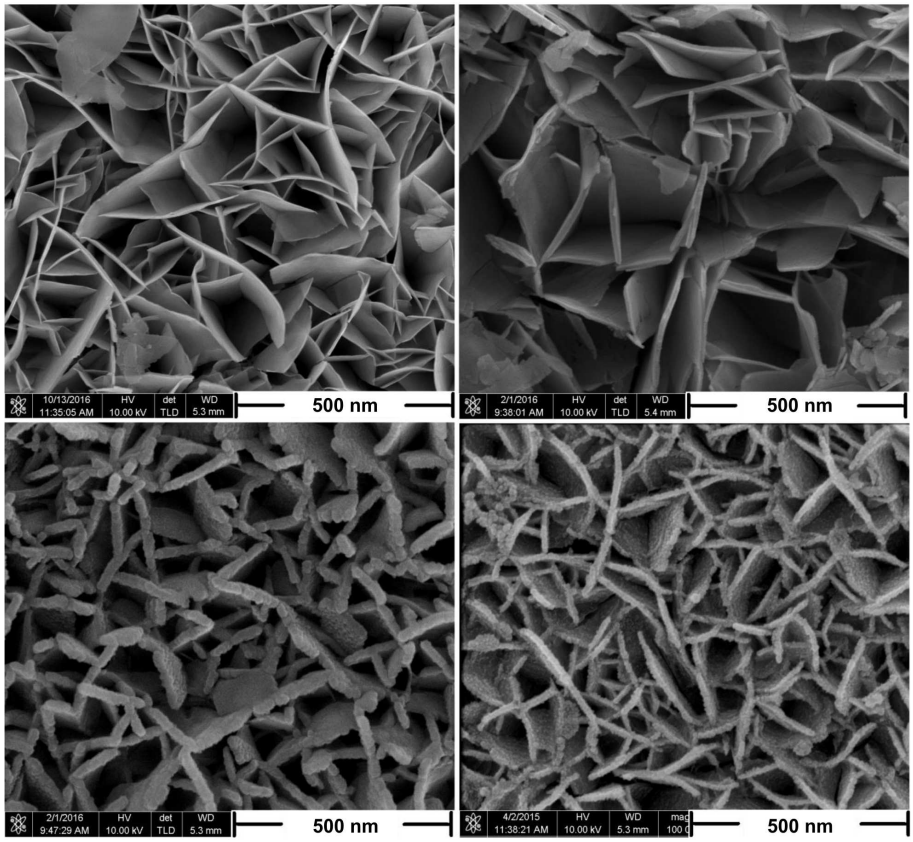

Fig. 2. FESEM image of nanoflakes in the samples for the samples as-grown (*a*) and annealed at 200 (*b*), 300 (*c*), and 400° (*d*)

for the subsequently annealed samples. For the as-grown film sample pattern, the $Ni(OH)_2$ phase was identified with the peaks labelled according to the ICSD 00-014-0117 at 33.15°, 38.62°, 59.18°, 62.73°, and 72.68° corresponding to a hexagonal unit cell with parameters $a = 3.1260$ (Å), $b = 3.1260$ (Å), and $c = 4.6050$ (Å) and angles $\alpha = 90°$, $\beta = 90°$, and $\gamma = 120°$. The peak for a cubic ITO structure pattern has been identified for both as-grown and annealed samples with a peak orientation of (111) at $2\theta = 30.62°$.

Subsequently, for the annealed samples, the X-ray diffraction peak attributed to cubic NiO was detected and labeled according to the ICSD 00-047-1049 of NiO crystals with the lattice parameter a, b, and $c = 4.1771$ Å, with the angles of α, β, and $\gamma = 90$. The peaks obtained were at $2\theta = 37.25°$, 43.28°, and 62.88° with the preferential orientation of the films at (111), (200) and (220) respectively, with the highest peak intensity at (111). This shows the polycrystalline structure of NiO films after the annealing, without traces of the $Ni(OH)_2$ phase on the treated films, which confirms a complete transformation of $Ni(OH)_2$ to NiO. The peak at (111) appears well-defined with the highest intensity at an annealing temperature of 300 °C. The high intensity of peaks for the sample annealed at 300 °C can be due to the high degree of crystallinity caused by the annealing temperature and increases with the NiO orientation in thin films. The result indicates that the properties of a NiO nanostructured thin film are a function of the annealing temperature, with the highest modifications of NiO nanoflakes crystallite state at the 300 °C annealing temperature, which indicates an enhancement of the crystallinity of thin films and their better quality.

The crystal size (D) was estimated, by basing on the FWHM (full width at the half-maximum) peak

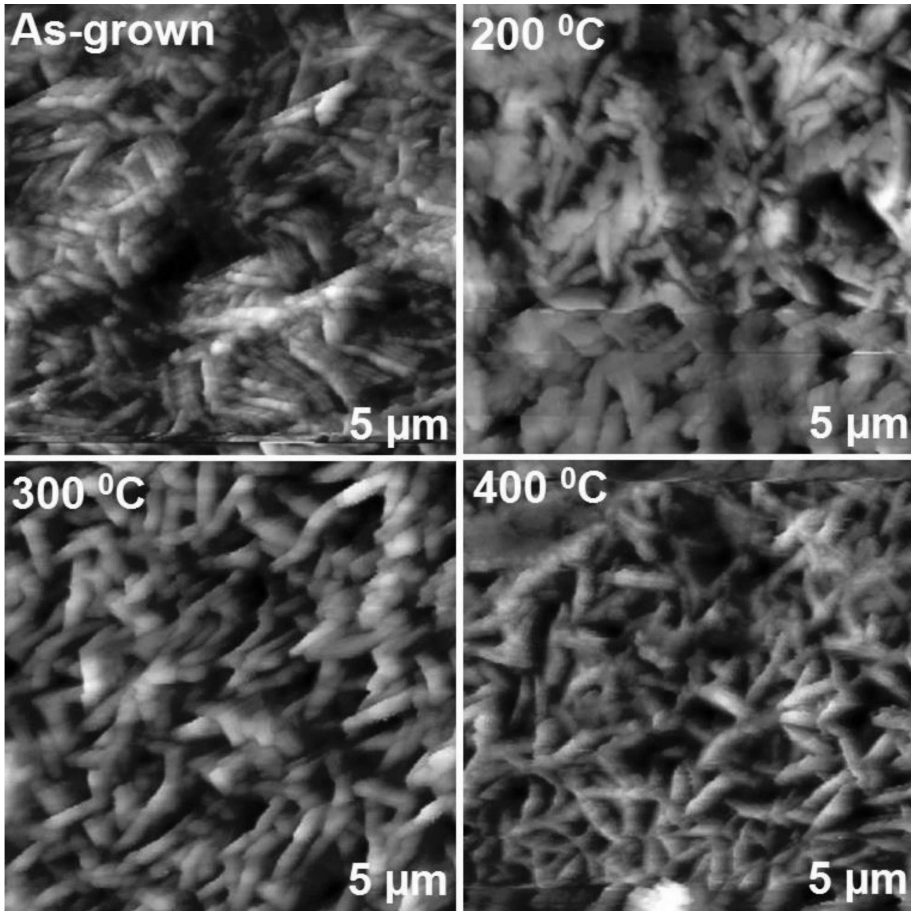

Fig. 3. Typical 2D AFM surface images for the as-grown $Ni(OH)_2$ sample and after the annealing at 200, 300, and 400 °C

position and the corresponding values of the obtained angle, by using Scherrer's equation (1)

$$D = \frac{0.9\lambda}{\beta \cos \theta}, \quad (1)$$

where λ is the X-ray wavelength, θ is the Bragg angle, and β is the line broadening at FWHM in radian.

Measurements of FESEM were made in order to investigate the morphological and structural properties of the chemically grown NiO thin films, as shown in Fig. 2. It is shown that the porous NiO nanostructured thin film was made up of interconnected net-like nanoflakes' wall with a width thickness of 10–70 nm of the samples. Their surface area increases with the annealing temperature. The diameter of pores ranges from 50 to 300 nm with an observable difference in the dimensions of thin film micro/nanostructures and the annealing at 300 °C shows the highest surface to volume ratio. The flakes wall appears to have a rough surface depending on the annealing temperature. The high porous nanostructure, high surface roughness and high surface to volume ratio can be an important factor that offers an easy access of ions to the surface reaction in chemical sensor device applications [22]. The sample annealed at 300 °C appears to have the highest quality by the FESEM results, which is an important factor for sensor devices.

The atomic and weight ratio of oxygen and nickel atom for the annealing sample shows the non-stoichiometric value of the two elements that characterize the state of a *p*-type semiconductor behavior, which is determined from the energy-dispersive spectroscopy (EDS) spectrum, as shown in Table 1.

The nanoporous NiO morphological study of the thin film's synthesis at different annealing temperatures was carrued out, by using AFM. Typical 2D AFM images of the as-grown $Ni(OH)_2$ and NiO thin films grown at a variable temperature are shown in Fig. 3. The mean roughnesses for $NiO/Ni(OH)_2$ were deduced from the AFM result, as shown in Table 2. It can be noted that the thin film roughness depends on the annealing temperature with the highest thin film roughness of 47.90 nm at 300 °C. Figure 4 is a plot of the absorbance against the wavelength for the thin-film deposited annealed samples with corresponding optical band gap energy. The optical band gap was obtained, by using the Tauc relation [23]

$$\alpha h\upsilon = B(h\upsilon - E_g)^{\gamma}, \tag{2}$$

where α is the absorption coefficient, E_g is the optical band gap energy, h is the Planck's constant, υ is the incident photon frequency, B is the constant known as the parameter of band tailing, and γ is the index. The index can have different values depending on the transition: 2 for an indirect allowed transition, 1/2 for a direct allowed transition, 3 for an indirect forbidden transition, and 1/3 for a direct forbidden transition. The band gaps of the thin-film samples were estimated by plotting $(\alpha h\upsilon)^2$ versus $h\upsilon$, as shown in the Fig. 4 insets with the linear

Table 1. **Weight and atomic percentages of the annealed and as-grown samples obtained with the use of the EDS spectrum**

Sample	As-grown		200°		300°		400°	
	Element							
	O	Ni	O	Ni	O	Ni	O	Ni
Atomic %	60.23	38.77	63.15	36.85	50.16	49.84	53.26	46.84
Weight %	29.51	70.49	32.16	67.94	21.35	78.65	23.79	76.21

Table 2. **Root mean square roughness *R*, lattice strain, and mean crystal size of as-grown $Ni(OH)_2$ and NiO thin films obtained from the AFM analysis**

Sample	As-grown	200°	300°	400°
Roughness (nm)	36.3	39.2	47.9	47.3
Mean crystal size (nm)	7.62	9.85	19.84	14.34
Lattice strain	0.135	0.110	0.043	0.072

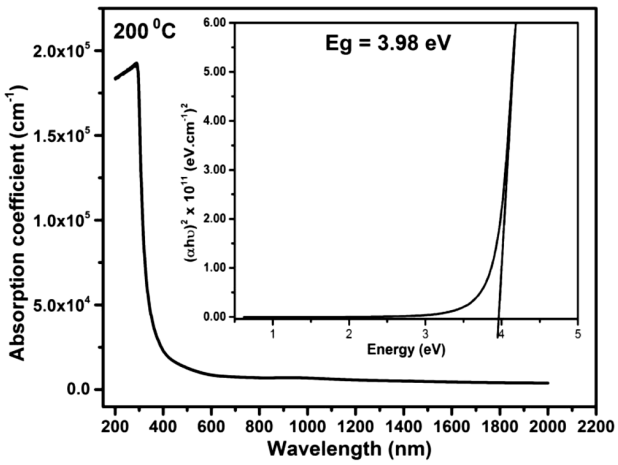

a

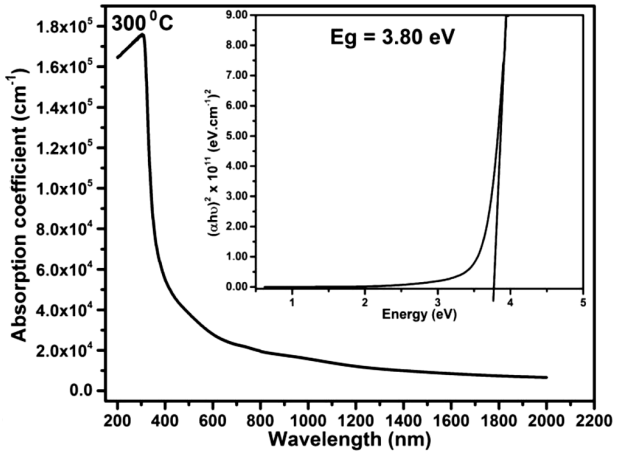

b

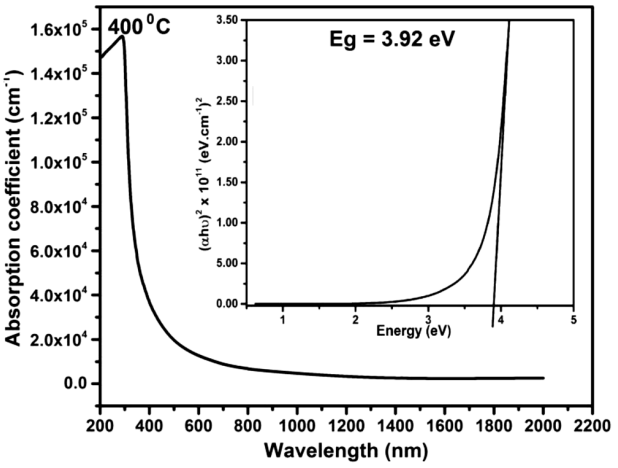

c

Fig. 4. Optical band gap energy of NiO at different temperatures

portion near the absorption edge onset and were extrapolated to the band gap energy x-axis. From the result, it can be seen that the indirect allowed transition of the system was followed, and the values of band gaps of the samples annealed at 200, 300, and 400 °C were found to be 3.98, 3.80, and 3.92 eV. The 300 °C sample appears with lower band gap due to its larger crystal size as a result of its higher crystallinity from XRD.

4. Conclusion

Nickel oxide thin films with nanoflakes are synthesized on ITO/glass substrates by an annealing treatment at variable temperatures of 200, 300, and 400 °C. The annealed sample appears to have a total transformation temperature of $Ni(OH)_2$ to NiO from the obtained characterization result of XRD. The FE-SEM analysis indicates that the nanoflake structure of NiO grown at 300 °C appears with the highest surface area and quality, and the EDS results prove to show the non-stoichiometric behavior of *p*-type NiO semiconductor due to the excess of oxygen. The XRD analysis shows that the NiO nanoflakes possess an orientation with cubic structure with the highest intensity of peaks and crystallinity at 300 °C for the (111) lattice. Likewise, the AFM result shows the highest roughness of the thin film sample annealed at 300 °C. The optical band gap of the UV-Vis measurement shows a lower value for 300 °C due to the highest crystallinity from XDR. Hence, in conclusion, the characterization result indicates that the optimum annealing temperature for the synthesis of NiO nanoflakes with the highest thin film quality, being the best for applications such as in biosensors and chemical sensors, is 300 °C.

The authors would wish to show their gratitude to Universiti Sains Malaysia together with GOT Incentive Grant 1001/PFIZIK/822055 and Nano-optoelectronics research and technology laboratory, School of Physics for the great support of this work.

1. C. Rovelli, L. Smolin. Spin networks and quantum gravity. *Phys. Phys. D* **52**, 5743 (1995).
2. B.W. Shore. *The Theory of Coherent Atomic Excitation* (Wiley, 1990) [ISBN: 978-0471524175].
3. N. Sattarahmady, H. Heli, R.D. Vais. An electrochemical acetylcholine sensor based on lichen-like nickel oxide nanostructure. *Biosens. Bioelectron.* **48**, 197 (2013).
4. S. Pereira, A. Gonçalves, N. Correia, J. Pinto, L. Pereira, R. Martins, E. Fortunato. Electrochromic behavior of NiO thin films deposited by e-beam evaporation at room temperature. *Sol. Energy Mater. Sol. Cells* **120**, 109 (2014).
5. F.I. Dar, K.R. Moonoosawmy, M. Es-Souni. Morphology and property control of NiO nanostructures for supercapacitor applications. *Nanoscale Res. Lett.* **8**, 363 (2013).
6. H. Pang, Q. Lu, Y. Zhang, Y. Li, F. Gao. Selective synthesis of nickel oxide nanowires and length effect on their electrochemical properties. *Nanoscale* **2**, 920 (2010).
7. L. Watkins. Development of non-noble catalysts for hydrogen and oxygen evolution in alkaline polymer electrolyte membrane electrolysis. *Newcastle Univ.* **9**, 204 (2013).
8. Z.H. Ibupoto, K. Khun, M. Willander. Development of a pH sensor using nanoporous nanostructures of NiO. *J. Nanosci. Nanotechnol.* **14**, 6699 (2014).
9. S. Sriram, A. Thayumanavan. Structural, optical and electrical properties of NiO thin films prepared by low cost spray pyrolysis technique. *Int. J. Mater. Sci. Eng.* **1**, 118 (2014).
10. D.S. Dalavi, M.J. Suryavanshi, D.S. Patil, S.S. Mali, A.V. Moholkar, S.S. Kalagi, S.A. Vanalkar, S.R. Kang, J.H. Kim, P.S. Patil. Nanoporous nickel oxide thin films and its improved electrochromic performance: Effect of thickness. *Appl. Surf. Sci.* **257**, 2647 (2011).
11. B.D.L. García-González, R. Aparicio. Sensors?: From biosensors to the electronic nose. *Grasas y Aceites* **53**, 96 (2002).
12. G. Bodurov, T. Ivanova, K. Gesheva. Technology and application of transition metal oxide of W–V–O as functional layers and NiO thin films as counter electrode material in electrochromic "smart windows". *Phys. Procedia* **46**, 149 (2013).
13. W.L. Jang, Y.M. Lu, W.S. Hwang, C.L. Dong, P.H. Hsieh, C.L. Chen, T.S. Chan, J.F. Lee. A study of thermal decomposition of sputtered NiO films. *Europhys. Lett.* **96**, 37009 (2011).
14. K. Zhang, C. Rossi, P. Alphonse, C. Tenailleau. Synthesis of NiO nanowalls by thermal treatment of Ni film deposited onto a stainless steel substrate. *Nanotechn.* **19**, 155605 (2008).
15. S.F. Oboudi, N.F. Habubi, G.H. Mohamed, S.S. Chiad. Composition and optical dispersion characterization of nanoparticles ZnO–NiO thin films?: Effect of annealing temperature. *Inter. Lette. Chem., Phys. Astron.* **8**, 78 (2013).
16. L. Li, K.S. Hui, K.N. Hui, H.W. Park, D.H. Hwang, S. Cho, S.K. Lee, P.K. Song, Y.R. Cho, H. Lee, Y.G. Son, W. Zhou. Synthesis and characterization of NiO-doped *p*-type AZO films fabricated by sol–gel method. *Mater. Lett.* **68**, 283 (2012).
17. C. Li, S. Liu. Preparation and characterization of $Ni(OH)_2$ and NiO mesoporous nanosheets. *J. Nanomater.* **2012**, 1 (2012).

18. S.M. Karadeniz, A.E. Ekinci, F.N. Tuzluca, M. Ertuprul. Properties of NiO thin films prepared by chemical spray pyrolysis using $NiSO_4$ precursor solution. *Asian J. Chem.* **24**, 1765 (2012).
19. S.-Y. Park, H.-R. Kim, Y.-J. Kang, D.-H. Kim, J.-W. Kang. Organic solar cells employing magnetron sputtered *p*-type nickel oxide thin film as the anode buffer layer. *Sol. Energy Mater. Sol. Cells* **94**, 2332 (2010).
20. Y. Lin, T. Xie, B. Cheng, B. Geng, L. Zhang. Ordered nickel oxide nanowire arrays and their optical absorption properties. *Chem. Phys. Lett.* **380**, 521 (2003).
21. X. Xia, J. Tu, X. Wang, C. Gu, X. Zhao. Hierarchically porous NiO film grown by chemical bath depositionvia a colloidal crystal template as an electrochemical pseudocapacitor material. *J. Mater. Chem.* **21**, 671 (2011).
22. M.E.G. Lyons, A. Cakara, P. O'Brien, I. Godwin, R.L. Doyle. Redox, pH sensing and electrolytic water splitting properties of electrochemically generated nickel hydroxide thin films in aqueous alkaline solution. *Int. J. Electrochem. Sci.* **7**, 11768 (2012).
23. M.A. Vidales-Hurtado, A. Mendoza-Galvan. Electrochromism in nickel oxide-based thin films obtained by chemical bath deposition. *Solid State Ionics* **179**, 2065 (2008).
24. A.I. Inamdar, Y. Kim, S.M. Pawar, J.H. Kim, H. Im, H. Kim. Chemically grown, porous, nickel oxide thin-film for electrochemical supercapacitors. *J. Power Sources* **196**, 2393 (2011).
25. S.H. Basri, M. Arif, M. Sarjidan, W. Haliza, A. Majid. Structural and optical properties of nickel-doped and undoped zinc oxide thin films deposited by sol-gel method. *Adv. Mater. Res.* **895**, 250 (2014).

Received 05.06.17

Д. Абубакар, Н. Махмуд, Ш. Махмуд

ДОСЛІДЖЕННЯ СТРУКТУРИ І ОПТИЧНИХ ВЛАСТИВОСТЕЙ NiO НАНОЛУСОЧОК. ВИРОЩУВАННЯ ТОНКИХ ПЛІВОК $Ni(OH)_2$ МЕТОДОМ ХІМІЧНОГО ОСАДЖЕННЯ

Р е з ю м е

Методом хімічного осадження вирощені пористі нанолусочки окису нікелю NiO. На підкладці оксид індію-олова/скло отримані тонкі плівки і піддані відпалу при змінній температурі в печі. Вивчено та проаналізовано їх структуру, оптичні властивості і морфологію поверхні. Методом емісійної растрової електронної мікроскопії показано присутність нанолусочок у структурі $NiO/Ni(OH)_2$ тонких плівок. Розміри нанолусочок збільшуються з ростом температури відпалу. Знайдено, що найбільшу площу поверхні має зразок, вирощений при 300 °C. Результати енергодисперсійної спектроскопії показують нестехіометрію атомного відношення зразка, що відповідає *p*-типу NiO тонкої плівки. Методом атомної силової спектроскопії знайдено, що зразок, вирощений при 300 °C, має найбільшу шорсткість (47,9 нм). Рентгеноструктурний аналіз показує, що NiO нанолусочки мають кубічну структуру з піками орієнтації (111), (200), і (220). Це особливо чітко проявляється при 300 °C. Рентгеноструктурний аналіз також показує відсутність $Ni(OH)_2$ піка при відпалі. Вимірювання в ультрафіолеті і видимому світлі дають малу ширину забороненої зони 3,80 еВ для 300 °C через високу кристалічність. Ця температура оптимальна для синтезу NiO нанолусочок високої якості, що важливо для їх застосування в сенсорах.